Communication

Charting the Complete Thermodynamic Landscape of Gas Adsorption for a Responsive Metal−Organic Framework

Ruben Goeminne, Simon Krause, Stefan Kaskel, Toon Verstraelen,* and Jack D. Evans*

Read Online

ACCESS | Metrics & More | Article Recommendations | Supporting Information

ABSTRACT: New nanoporous materials have the ability to revolutionize adsorption and separation processes. In particular, materials with adaptive cavities have high selectivity and may display previously undiscovered phenomena, such as negative gas adsorption (NGA), in which gas is released from the framework upon an increase in pressure. Although the thermodynamic driving force behind this and many other counterintuitive adsorption phenomena have been thoroughly investigated in recent years, several experimental observations remain difficult to explain. This necessitates a comprehensive analysis of gas adsorption akin to the conformational free energy landscapes used to understand the function of proteins. We have constructed the complete thermodynamic landscape of methane adsorption on DUT-49. Traversing this complex landscape reproduces the experimentally observed structural transitions, temperature dependence, and the hysteresis between adsorption and desorption. The complete thermodynamic description presented here provides unparalleled insight into adsorption and provides a framework to understand other adsorbents that challenge our preconceptions.

Advanced porous materials can deliver exciting developments to industrial processes[1] and the flexibility of porous adsorbents could address complex separations similar to biological systems.[2] For example, extreme changes in adsorption behavior produce improved selectivity, storage capacity, and thermal management.[3−5] Responsive adsorbents, such as metal−organic frameworks (MOFs), can significantly change pore structure and volume in response to external stimuli such as pressure, temperature, gas adsorption or light absorption.[6]

One particularly exciting MOF that exhibits negative gas adsorption (NGA) is DUT-49. This MOF undergoes a structural transition associated with a 50% contraction of the unit cell upon increasing methane gas pressure, resulting in spontaneous desorption of methane.[7] This leads to pressure amplification in a closed system, opening the door to new applications.[8] The lack of thermodynamic understanding of the NGA phenomenon has motivated a number of computational studies.[9,10] However, efforts have mostly relied on two-state models that are unable to capture the complete phase-space during adsorption and desorption.[11]

The most appropriate description of the thermodynamics of responsive frameworks under gas adsorption is provided by the osmotic ensemble. Simulations in this ensemble impose a chemical potential of the adsorbed fluid (μ), a mechanical pressure (p), and a temperature (T). Under these conditions, the equilibrium framework minimizes the osmotic potential (Ω) through structural relaxation, changes in cell shape and volume, and adsorption of guest molecules.[12] However, atomistic simulations within the osmotic ensemble remain challenging because dynamics must be combined with particle insertion/deletion, limiting its application to a handful of systems.[13,14] Descriptions of the osmotic potential are often achieved through analytical treatment of gas adsorption.[15] This

can ascertain the relative stability of two distinct and porous phases.[16] For example, the process of "breathing" between an open (*op*) and contracted porous phase (*cp*), such as that observed for MIL-53,[17] can be understood by their difference in osmotic potential, $\Omega_{op} - \Omega_{cp}$ (Figure 1).[12] The difference in osmotic potential reveals which phase represents the global thermodynamic equilibrium as a function of gas pressure.[18] However, this methodology is not sufficient to describe NGA as it must involve metastable states.[7] Moreover, the
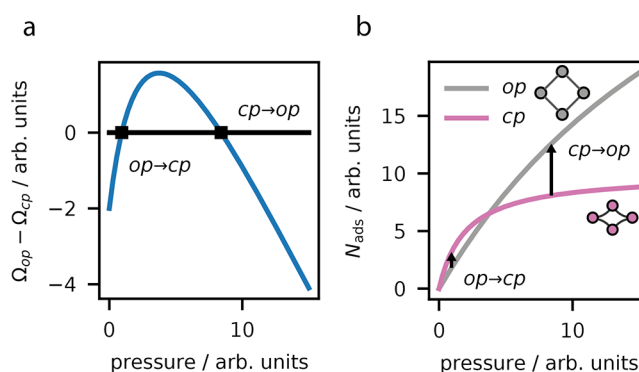

Figure 1. Osmotic potential (a) applied to transitions between two phases (*op* and *cp*) of an adsorbent. This can describe the "breathing" adsorption phenomenon (b).

experimentally observed hysteresis and temperature dependence of NGA cannot be reproduced by simply considering the difference in osmotic potential.[19] Experiments demonstrate that the *op* to *cp* transition at 90 K produces a much smaller NGA step than 120 K, whereas at 150 K, no transitions are observed.[19] To explain this temperature dependence and other complex adsorption processes, knowledge of not only the osmotic potential but also the osmotic barriers that exist between phases that act to prevent transformations, are required.

Free-energy landscapes of chemical reactions and conformational dynamics are expressed in terms of collective variables; similarly, barriers of "breathing" MOFs in the osmotic ensemble appear at specific cell volumes. We employed molecular simulations to treat the cell volume (V) as a "collective variable" in the osmotic ensemble. The osmotic potential, as a function of volume, reveals the (meta)stable states of interest and the barriers between them for any set of thermodynamic parameters μ, p, and T. With this method, detailed landscapes of the osmotic potential, as a function of cell volume of DUT-49 and methane gas pressure, have been computed at 90, 120, and 150 K. This complete thermodynamic analysis provides comprehensive insight into phase stability under adsorption.

We employed a force field derived from ab initio data of the inorganic and organic units of the DUT-49 framework[10] with the TraPPE[20] parametrization of methane. In our hybrid MC[14,21−23] simulations, molecular dynamics (MD) trajectories in the (N, V, $\sigma_a = 0$, T) ensemble are new moves in a grand canonical Monte Carlo scheme. The MD simulations impose a fixed volume V and anisotropic contribution σ_a to the total stress tensor $\sigma = P\mathbf{1} + \sigma_a$,[24] allowing the cell shape to adapt to the fluctuating number of adsorbates resulting in flexible-host adsorption isotherms, $N_{guest}(N_{host}, \mu, \sigma_a = 0, T; V)$. Isotherms were calculated for a series of unit cell volumes between 40 and 110 nm³ with a spacing of 2 nm³ (Figure 2). Subsequently, the flexible-host isotherms were used to construct the osmotic potential as eq 1.

$$\Omega(N_{host}, p, \sigma_a = 0, T; V) = F_{host}(N_{host}, T; V) + pV$$
$$- \int_{-\infty}^{\mu(p,T)} N_{guest}(N_{host}, \mu', \sigma_a = 0, T; V) \, d\mu' \quad (1)$$

The empty-host free energy F_{host} was obtained by thermodynamic integration of the internal pressure, extracted from MD simulations of the empty framework in the (N, V, $\sigma_a = 0$, T) ensemble at different unit cell volumes at 90, 120, and 150 K. The free energy was chosen to be 0 kJ mol⁻¹ in the *op* phase at a unit cell volume of 104 nm³, comparable to the experimentally observed unit cell volume of 100 nm³.[7] This produces a meaningful comparison of the empty-host free energy (and thus osmotic potential). Simulations were performed between 46 and 75 values of gas pressure and the chemical potential at each temperature and gas pressure was calculated with the Peng−Robinson equation of state.[25] The above approach produces the osmotic potential at different methane gas pressures and cell volumes. The osmotic landscape is shown relative to the *op* phase at each gas pressure in Figure 2 to highlight differences between the phases. In contrast to previous approaches (Figure 1a), this surface offers a tremendous amount of additional information.

To clearly outline the effect of osmotic barriers on gas adsorption, we can chart paths[26] on the osmotic landscape that
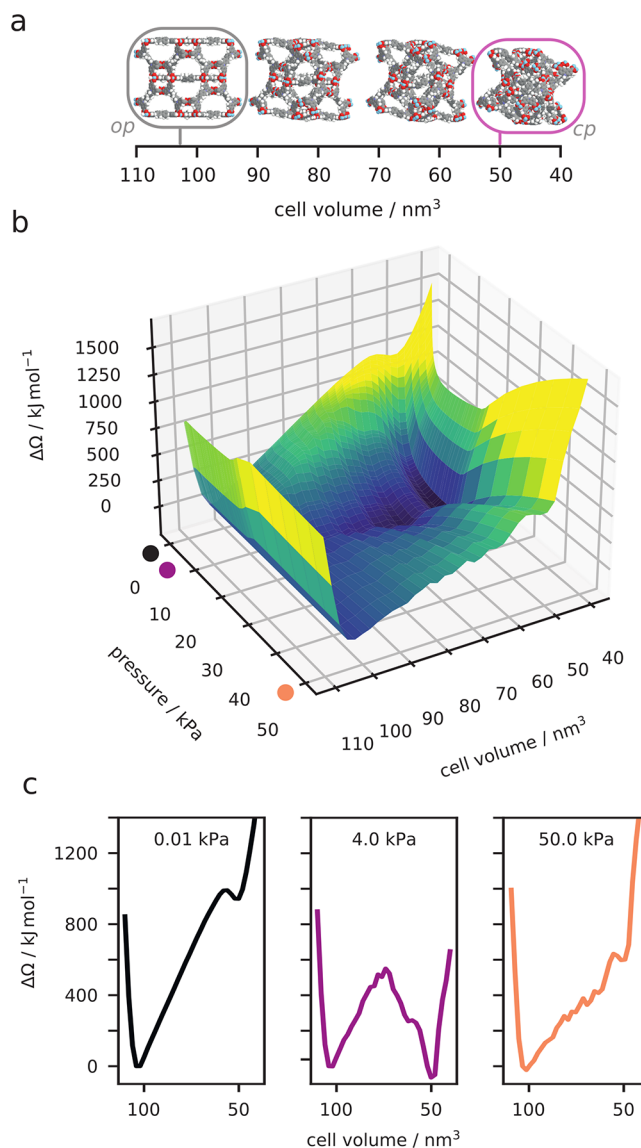

Figure 2. Computed osmotic surface of methane adsorption on DUT-49 at 120 K, as a function of unit cell volume (a) and methane gas pressure (b). Examples of the 1D osmotic surface at specific gas pressures (c).

are taken with adsorption and desorption along with the associated amount adsorbed. Figure 3a−c shows the path along which the system is in global thermodynamic equilibrium at each gas pressure, i.e., the path of lowest osmotic potential. Alternatively, Figure 3d−f shows the kinetic path along which transitions can occur only when the osmotic barrier between phases disappears. However, as thermal fluctuations can allow the crossing of barriers, a transition was noted when the barrier was reduced to 15 k_BT. The same transitions are obtained for the computed 120 K surface when varying this value of "crossable" barriers between 0 and 25 k_BT. The appropriate value of barrier heights that can be crossed in typical time spans of experiments at a given temperature is difficult to obtain. For example, a fluctuation energy of 6 k_BT per unit cell was proposed for a gate-opening MOF.[27]

At zero gas pressure, the system begins at equilibrium in the *op* phase, where there is also a metastable *cp* phase (at 50 nm³). By increasing gas pressure, the *cp* phase is stabilized with respect to the *op* phase, until the difference in osmotic
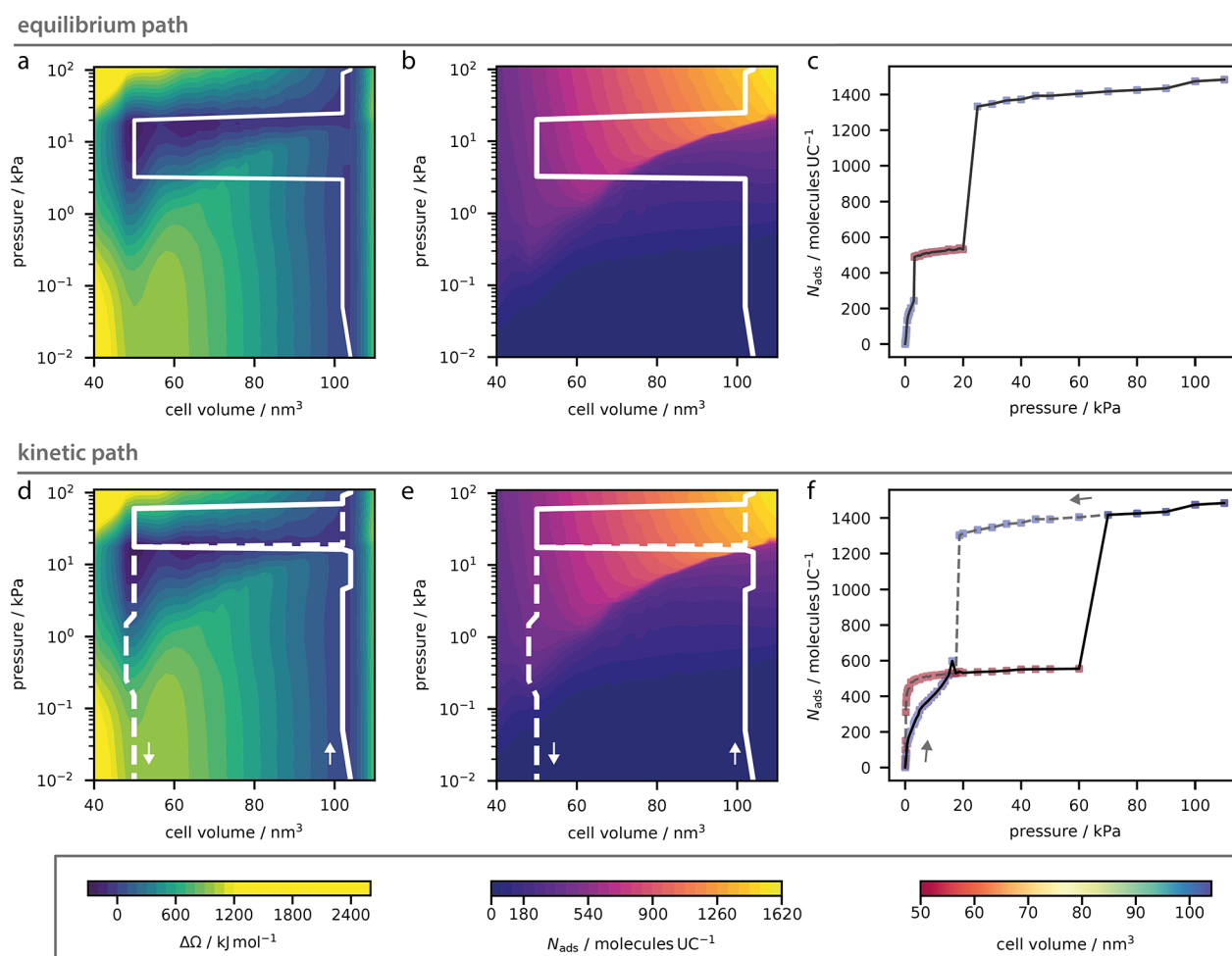
Figure 3. Osmotic potential (a) and the quantity adsorbed (b) surfaces of methane adsorption on DUT-49 at 120 K, with the thermodynamic equilibrium path, resulting in the equilibrium adsorption isotherm (c). The adsorption (solid line) and desorption (dashed line) path for kinetically accessible states on the same surfaces (d and e) that produce the adsorption isotherm (f).

potential between both phases vanishes at a gas pressure of 3.25 kPa. At this point, a transition occurs along the equilibrium path to the *cp* phase (Figure 3a). This contraction produces an increase in amount adsorbed, a step of 236 molecules per unit cell (molecules UC^{-1}). Conversely, no transitions occur along the kinetic path at this pressure, as a barrier between the *op* and *cp* phase of 591 kJ mol^{-1} remains. This barrier only vanishes at a gas pressure of 17.5 kPa, at which the *op* → *cp* transition occurs, associated with a NGA step of 86 molecules UC^{-1}. This predicted transition pressure is remarkably close to the observed value of 25 kPa. Although the predicted NGA step is underestimated compared to experiments (102 molecules UC^{-1}), the observation that the NGA phenomenon can be captured by atomistic simulation is remarkable in itself. On further increasing the gas pressure to 25 kPa, the *op* phase becomes the equilibrium phase, shown by the second transition in Figure 3b. However, the barrier between these phases only disappears at a higher gas pressure of 70 kPa (Figure 3d).

Just as a trajectory can be walked toward increasing gas pressures, the same process can be done in reverse to track desorption. The same path is obtained for the equilibrium path, the experimentally observed hysteresis is absent with this approach. Kinetic paths are different in adsorption and desorption. Osmotic potential energy barriers during desorp-

tion, which prevent an *op* → *cp* transition, only disappear when the gas pressure decreases to 17.5 kPa. This prediction of an *op* → *cp* transition during desorption at a gas pressure similar to that of the *op* → *cp* transition during adsorption is in agreement with experiments, attributed to the flat osmotic potential landscape over the entire volume range at this pressure. Interestingly, on decreasing the gas pressure further, it is predicted from this surface that the framework remains locked into the *cp* phase, as observed experimentally. This is due to the barrier surrounding the *cp* local minimum of the osmotic potential landscape at low gas pressures.

The structural transitions derived from the kinetic pathway during adsorption and desorption at 90 K agree quantitatively with reported in situ powder X-ray diffraction experiments.[7] The presence of intermediate phases between the *op* and *cp* phases at approximately 2 kPa are reproduced, evidencing the flatness of osmotic landscape at this gas pressure.

Recently, we reported methane adsorption on DUT-49 for the range 91−190 K, observing a non-monotonic trend of NGA amount with temperature and a distinct temperature window.[19] To provide insight into this trend, simulations were completed for three temperatures (90, 120, and 150 K). The difference in osmotic potential energy between the *op* and *cp* phases (corresponding to 104 and 50 nm^3, respectively) is directly computed from these simulations, as well as the

osmotic potential energy barrier from *op* to *cp* (Figure 4a). The pressure window for stability of the *cp* phase (where $\Omega_{op} - \Omega_{cp}$
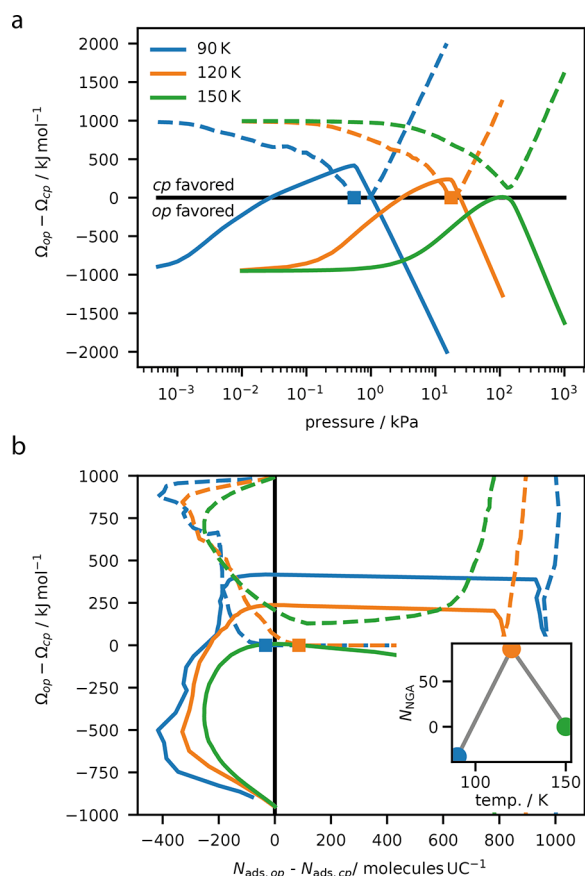

Figure 4. Difference in osmotic potential between *op* and *cp* phases (solid lines) and the barrier height between these phases (dashed lines) (a). The same difference in osmotic potential and barriers displayed with respect to the difference in amount adsorbed (b). The point where the osmotic potential barrier disappears is marked by a square. Predicted amount of NGA in units of molecules UC^{-1} (b, inset).

> 0) is significantly affected by temperature. This results in the $op \rightarrow cp$ phase transitions becoming unfavorable at 150 K, in line with the absence of experimentally observed phase transitions at this temperature and beyond.[19] We can alternatively consider these trends with respect to the difference in adsorbed amount in the *op* and *cp* phases (Figure 4b), representing the amount of NGA (N_{NGA}). The barrier present at 90 K disappears before the isotherm crossing point, implying that NGA is suppressed, whereas at 120 K, the barrier only disappears after the *op* state has more methane adsorbed than the *cp* state, necessitating the release of gas and the NGA step. By considering the amount adsorbed in each of the phases when the osmotic potential barrier for the $op \rightarrow cp$ transition disappears, we can predict the amount of NGA (Figure 4b, inset). This qualitative description outlines how NGA must be a function of not only the difference in osmotic potential but also the barrier to produce a temperature window.

We have outlined an approach to investigate a responsive gas adsorption process using atomistic simulations to create an osmotic potential surface. Roaming this surface using equilibrium or kinetic trajectories produces very different

isotherms. It is only by considering a kinetic pathway that accounts for osmotic potential barriers that the salient features of complex adsorption processes are produced. We used this model to understand the effects of temperature, demonstrating the previously poorly understood non-monotonic trend of NGA magnitude. The presented methodology enables ab initio prediction of NGA and permits investigation of similar counterintuitive adsorption processes. This is an important step toward predicting the evolution of conformational energy landscapes of flexible porous materials upon guest adsorption.[28] In particular, this new insight into the barriers present in responsive adsorption processes is of utmost importance for the intended application of these materials in kinetic selectivity and recognition. Many separation process are emphasized for flexible porous materials, but hysteresis is rarely addressed and poorly understood.[29] This approach highlights how desorption can access an entirely different pathway than adsorption. Flexible systems can wander beyond equilibrium, and it is only by mapping the complete energy surface that we can understand these unique adsorption phenomena and pave the way for new adsorbent technologies.

■ ASSOCIATED CONTENT

Ⓢ Supporting Information

The Supporting Information is available free of charge at https://pubs.acs.org/doi/10.1021/jacs.1c00522.

> Details of the classical potentials, the simulation procedures and additional figures of the computed surfaces and adsorption isotherms (PDF)
>
> Movie showing the osmotic landscape at 120 K (MP4)

■ AUTHOR INFORMATION

Corresponding Authors

Toon Verstraelen − *Center for Molecular Modeling, Ghent University, 9052 Zwijnaarde, Belgium;* ⓘ orcid.org/0000-0001-9288-5608; Email: toon.verstraelen@ugent.be

Jack D. Evans − *Department of Inorganic Chemistry, Technische Universität Dresden, 01062 Dresden, Germany;* ⓘ orcid.org/0000-0001-9521-2601; Email: jack.evans@tu-dresden.de

Authors

Ruben Goeminne − *Center for Molecular Modeling, Ghent University, 9052 Zwijnaarde, Belgium*

Simon Krause − *Stratingh Institute for Chemistry, Faculty of Mathematics and Natural Sciences, University of Groningen, 9747 AG Groningen, The Netherlands;* ⓘ orcid.org/0000-0001-9504-8514

Stefan Kaskel − *Department of Inorganic Chemistry, Technische Universität Dresden, 01062 Dresden, Germany*

Complete contact information is available at:
https://pubs.acs.org/10.1021/jacs.1c00522

Notes

The authors declare no competing financial interest.

■ REFERENCES

(1) Davis, M. E. Ordered porous materials for emerging applications. *Nature* **2002**, *417*, 813−821.

(2) Rabone, J.; Yue, Y.-F.; Chong, S. Y.; Stylianou, K. C.; Bacsa, J.; Bradshaw, D.; Darling, G. R.; Berry, N. G.; Khimyak, Y. Z.; Ganin, A. Y.; Wiper, P.; Claridge, J. B.; Rosseinsky, M. J. An Adaptable Peptide-Based Porous Material. *Science* **2010**, *329*, 1053−1057.

(3) Mason, J. A.; Oktawiec, J.; Taylor, M. K.; Hudson, M. R.; Rodriguez, J.; Bachman, J. E.; Gonzalez, M. I.; Cervellino, A.; Guagliardi, A.; Brown, C. M.; Llewellyn, P. L.; Masciocchi, N.; Long, J. R. Methane storage in flexible metal−organic frameworks with intrinsic thermal management. *Nature* **2015**, *527*, 357−361.

(4) Nijem, N.; Wu, H.; Canepa, P.; Marti, A.; Balkus, K. J.; Thonhauser, T.; Li, J.; Chabal, Y. J. Tuning the gate opening pressure of Metal-Organic Frameworks (MOFs) for the selective separation of hydrocarbons. *J. Am. Chem. Soc.* **2012**, *134*, 15201−15204.

(5) Zhang, J.-P.; Zhou, H.-L.; Zhou, D.-D.; Liao, P.-Q.; Chen, X.-M. Controlling flexibility of metal−organic frameworks. *National Science Review* **2018**, *5*, 907−919.

(6) Coudert, F.-X. Responsive Metal-Organic Frameworks and Framework Materials: Under Pressure, Taking the Heat, in the Spotlight, with Friends. *Chem. Mater.* **2015**, *27*, 1905−1916.

(7) Krause, S.; Bon, V.; Senkovska, I.; Stoeck, U.; Wallacher, D.; Többens, D. M.; Zander, S.; Pillai, R. S.; Maurin, G.; Coudert, F.-X.; Kaskel, S. A pressure-amplifying framework material with negative gas adsorption transitions. *Nature* **2016**, *532*, 348−352.

(8) Bon, V.; Krause, S.; Senkovska, I.; Grimm, N.; Wallacher, D.; Többens, D. D.; Kaskel, S. Massive Pressure Amplification by Stimulated Contraction of Mesoporous Frameworks. *ChemRxiv*, December 1, 2021, ver. 3. DOI: 10.26434/chemrxiv.12758015.v3 (accessed 2021−03−01).

(9) Evans, J. D.; Bocquet, L.; Coudert, F.-X. Origins of Negative Gas Adsorption. *Chem.* **2016**, *1*, 873−886.

(10) Vanduyfhuys, L.; Van Speybroeck, V. Unraveling the thermodynamic conditions for negative gas adsorption in soft porous crystals. *Commun. Phys.* **2019**, *2*, 102.

(11) Krause, S.; Hosono, N.; Kitagawa, S. Chemistry of Soft Porous Crystals: Structural Dynamics and Gas Adsorption Properties. *Angew. Chem., Int. Ed.* **2020**, *59*, 15325−15341.

(12) Coudert, F. X.; Jeffroy, M.; Fuchs, A. H.; Boutin, A.; Mellot-Draznieks, C. Thermodynamics of guest-induced structural transitions in hybrid organic-inorganic frameworks. *J. Am. Chem. Soc.* **2008**, *130*, 14294−14302.

(13) Zang, J.; Nair, S.; Sholl, D. S. Osmotic ensemble methods for predicting adsorption-induced structural transitions in nanoporous materials using molecular simulations. *J. Chem. Phys.* **2011**, *134*, 184103.

(14) Rogge, S. M. J.; Goeminne, R.; Demuynck, R.; Gutiérrez-Sevillano, J. J.; Vandenbrande, S.; Vanduyfhuys, L.; Waroquier, M.; Verstraelen, T.; Van Speybroeck, V. Modeling Gas Adsorption in Flexible Metal−Organic Frameworks via Hybrid Monte Carlo/Molecular Dynamics Schemes. *Adv. Theory Simul.* **2019**, *2*, 1800177.

(15) Dunne, L. J.; Manos, G. Exact matrix treatment of an osmotic ensemble model of adsorption and pressure induced structural transitions in metal organic frameworks. *Dalton Transactions* **2016**, *45*, 4213−4217.

(16) Boutin, A.; Coudert, F.-X.; Springuel-Huet, M.-A.; Neimark, A. V.; Férey, G.; Fuchs, A. H. The Behavior of Flexible MIL-53(Al) upon CH4 and CO2 Adsorption. *J. Phys. Chem. C* **2010**, *114*, 22237−22244.

(17) Llewellyn, P. L.; Maurin, G.; Devic, T.; Loera-Serna, S.; Rosenbach, N.; Serre, C.; Bourrelly, S.; Horcajada, P.; Filinchuk, Y.; Férey, G. Prediction of the Conditions for Breathing of Metal Organic Framework Materials Using a Combination of X-ray Powder Diffraction, Microcalorimetry, and Molecular Simulation. *J. Am. Chem. Soc.* **2008**, *130*, 12808−12814.

(18) The gas pressure equals the mechanical pressure and also affects the chemical potential of the fluid.

(19) Krause, S.; Evans, J. D.; Bon, V.; Senkovska, I.; Coudert, F.-X.; Többens, D. M.; Wallacher, D.; Grimm, N.; Kaskel, S. The role of temperature and adsorbate on negative gas adsorption transitions of the mesoporous metal−organic framework DUT-49. *Faraday Discuss.* **2021**, *225*, 168−183.

(20) Martin, G. M.; Siepmann, J. I. Transferable Potentials for Phase Equilibria. 1. United-Atom Description of *n*-Alkanes. *J. Phys. Chem. B* **1998**, *102*, 2569.

(21) Faller, R.; de Pablo, J. J. Constant pressure hybrid molecular dynamics-Monte Carlo simulations. *J. Chem. Phys.* **2002**, *116*, 55−59.

(22) Banaszak, B. J.; Faller, R.; de Pablo, J. J. Simulation of the effects of chain architecture on the sorption of ethylene in polyethylene. *J. Chem. Phys.* **2004**, *120*, 11304−11315.

(23) Ghoufi, A.; Maurin, G. Hybrid monte carlo simulations combined with a phase mixture model to predict the structural transitions of a porous Metal-organic framework material upon adsorption of guest molecules. *J. Phys. Chem. C* **2010**, *114*, 6496−6502.

(24) Rogge, S. M. J.; Caroes, S.; Demuynck, R.; Waroquier, M.; Van Speybroeck, V.; Ghysels, A. The Importance of Cell Shape Sampling To Accurately Predict Flexibility in Metal−Organic Frameworks. *J. Chem. Theory Comput.* **2018**, *14*, 1186−1197.

(25) Peng, D.-Y.; Robinson, D. B. A New Two-Constant Equation of State. *Ind. Eng. Chem. Fundam.* **1976**, *15*, 59−64.

(26) Evans, J. D.; Krause, S.; Kaskel, S.; Sweatman, M. B.; Sarkisov, L. Exploring the thermodynamic criteria for responsive adsorption processes. *Chemical Science* **2019**, *10*, 5011−5017.

(27) Numaguchi, R.; Tanaka, H.; Watanabe, S.; Miyahara, M. T. Simulation study for adsorption-induced structural transition in stacked-layer porous coordination polymers: Equilibrium and hysteretic adsorption behaviors. *J. Chem. Phys.* **2013**, *138*, 054708.

(28) Katsoulidis, A. P.; Antypov, D.; Whitehead, G. F. S.; Carrington, E. J.; Adams, D. J.; Berry, N. G.; Darling, G. R.; Dyer, M. S.; Rosseinsky, M. J. Chemical control of structure and guest uptake by a conformationally mobile porous material. *Nature* **2019**, *565*, 213−217.

(29) Rahman, S.; Arami-Niya, A.; Yang, X.; Xiao, G.; Li, G. K.; May, E. F. Temperature dependence of adsorption hysteresis in flexible metal organic frameworks. *Commun. Chem.* **2020**, *3*, 186.

■ NOTE ADDED AFTER ISSUE PUBLICATION

This article was initially published with an incorrect copyright statement and was corrected on or around May 5, 2021.